Proc. Natl. Acad. Sci. USA
Vol. 88, pp. 7896–7900, September 1991
Cell Biology

Micromotion of mammalian cells measured electrically

(cell motility/fibroblast behavior/nanometer motions/electrical measurements)

IVAR GIAEVER AND CHARLES R. KEESE

School of Science, Rensselaer Polytechnic Institute, Troy, NY 12180-3590

Contributed by Ivar Giaever, May 16, 1991

ABSTRACT **Motility is a fundamental property of mammalian cells that normally is observed in tissue culture by time lapse microscopy where resolution is limited by the wavelength of light. This paper examines a powerful electrical technique by which cell motion is quantitatively measured at the nanometer level. In this method, the cells are cultured on small evaporated gold electrodes carrying weak ac currents. A large change in the measured electrical impedance of the electrodes is observed when cells attach and spread on these electrodes. When the impedance is tracked as a function of time, fluctuations are observed that are a direct measure of cell motion. Surprisingly, these fluctuations continue even when the cell layer becomes confluent. By comparing the measured impedance with a theoretical model, it is clear that under these circumstances the average motions of the cell layer of 1 nm can be inferred from the measurements. We refer to this aspect of cell motility as micromotion.**

Locomotion of cells in tissue culture has been widely observed, as many metazoan cells have the ability to crawl upon surfaces. This *in vitro* phenomena is thought to be an expression of a basic cellular mechanism involved in processes including wound healing, maintenance of cellular organization in tissues, surveillance for invading organisms, and development of the early embryo (1). Several recent studies have reported a link between the metastatic behavior of cancer cells and their motility in culture (2–4). Such correlations will be of significance both in understanding the metastatic process and in devising clinical measurements for prognosis and treatment of cancer. The detection of cell motility, however, has been a difficult and time consuming process. The simplest and most direct approaches involve microscopic observations of cells, usually with the aid of time lapse cameras. In recent years, these data are often image processed and analyzed by computer. This provides a direct measure of translation and other aspects of cell motion, but the procedure requires processing large volumes of data.

In this paper, we describe and analyze a means to electrically detect cell motion in tissue culture (5–7). In this method, cells are cultured on small gold electrodes evaporated on the bottom of standard tissue culture dishes and the system's impedance is followed with time. As the cells attach and spread on the electrode surface, they alter the effective area available for current flow causing as much as an 8-fold increase in the impedance of the system. After these initial changes, the impedance fluctuates with time.

In the past, we have shown that these fluctuations in impedance result from the motion of cells on the electrode. For example, treatment of fibroblasts with 10 μM cytochalasin B resulted in a nearly complete cessation of the impedance fluctuations (7). The mechanism involved seemed at first sight straightforward; as cells move on and off an electrode, the effective open area changes and with it the electrode impedance. The impedance fluctuations, however, continue as cell layers become confluent. To understand these results and the possible sources of the fluctuations, we have considered the interaction of cultured cells with the electrode surface in detail.

It is well known from interference reflection microscopy studies that cells in culture attach to the substratum by small foot-like projections leaving spaces or channels between the ventral side of the cell and the substratum (8). The amount of current flowing in these channels, and hence the impedance of the cell-covered electrode, will depend on the applied ac frequency. We have modeled this system and compared the calculated impedance values as a function of frequency with those measured for confluent layers of WI-38 and WI-38 VA13 cells. In addition, we have calculated to what degree changes in various cell parameters will affect impedance measurements.

MATERIALS AND METHODS

Tissue Culture. The fibroblast cell lines WI-38 and WI-38 VA13 were obtained from the American Type Culture Collection. All culturing was done under standard conditions of 37°C and 5% CO_2/95% air in Dulbecco's modified Eagle's medium (GIBCO) with 10% fetal bovine serum (GIBCO) and antibiotics.

Electrode Fabrication. The preparation of 60-mm polystyrene culture dishes containing gold electrodes deposited by vacuum evaporation has been described (6, 7). Each finished dish contained one large ($\approx$2 cm^2) and four small ($\approx 10^{-3}$ cm^2) electrodes.

Impedance Measurements. For impedance measurements, the electrode-containing dish was placed in an incubator and medium ($\approx$4 ml) was added over the electrodes. The large electrode and one of the small electrodes were connected to a phase-sensitive lock-in amplifier, and an ac signal was supplied through a 1-MΩ resistor (see Fig. 1). The measurement was generally made with a 4000-Hz ac source with an amplitude of 1.0 V. For frequencies scans shown in Fig. 3, however, the following ac frequencies and respective amplitudes were used: 22 Hz and 0.014 V, 44 Hz and 0.020 V, 88 Hz and 0.027 V, 176 Hz and 0.038 V, 352 Hz and 0.054 V, 704 Hz and 0.075 V, 1408 Hz and 0.105 V, 2816 Hz and 0.148 V, 5632 Hz and 0.207 V, 11,264 Hz and 0.289 V, 22,528 Hz and 0.405 V, 45,056 Hz and 0.557 V, 90,112 Hz and 0.794 V.

All connections were with coaxial cable to minimize any background noise. For cell measurements, the dish was inoculated with 2 ml of a cell suspension giving a concentration of 1×10^5 cells per cm^2 of available area. Cells were allowed to attach and spread for at least 24 hr before the impedance measurements reported in this paper were taken.

RESULTS AND DISCUSSION

Fig. 1 shows a schematic of the electrodes and the basic electrical setup used in these measurements. In this two-

The publication costs of this article were defrayed in part by page charge payment. This article must therefore be hereby marked "*advertisement*" in accordance with 18 U.S.C. §1734 solely to indicate this fact.

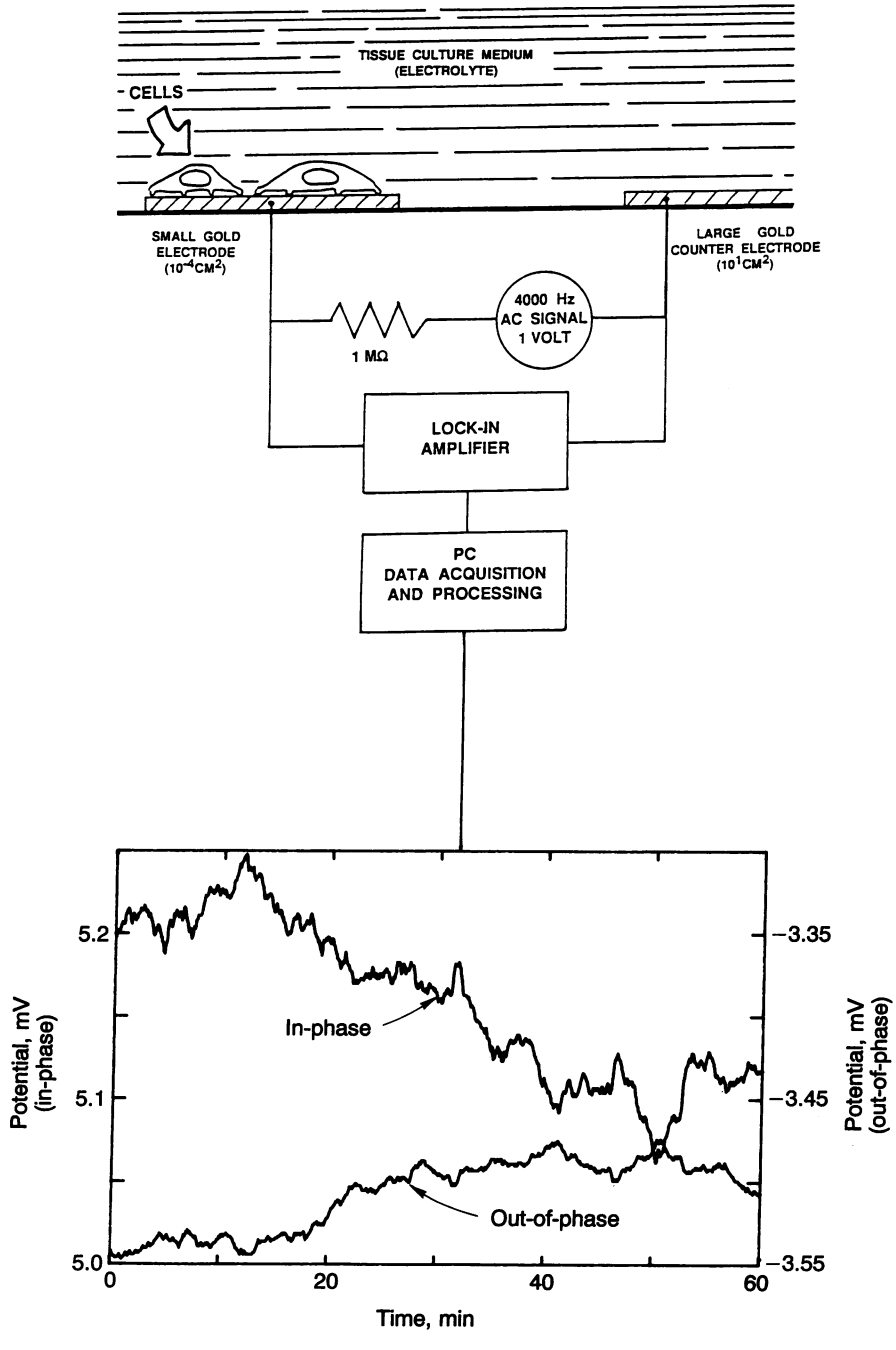

FIG. 1. Schematic of the experiment. Impedance of the small electrode is measured with a lock-in amplifier in series with a 1-MΩ resistor to obtain an approximate constant current source. The measured fluctuations in the real and imaginary voltage are displayed for a 1-hr experiment with confluent WI-38 VA13 fibroblasts using a 4-kHz 1-V source. The in-phase and out-of-phase voltage values are approximately proportional to the respective changes in resistance and capacitive reactance of a series RC circuit.

probe measurement, the resistance of the bulk tissue culture medium is in series with the impedance of the electrodes and will dominate the measurement except when an electrode is small. The solution resistance will then manifest itself as a spreading or constriction resistance that depends on the size of the electrode. As an example, for a circular disk electrode in a conducting medium of infinite extent, the constriction resistance varies as $\rho/2d$, where ρ is the resistivity of the medium and d is the diameter of the electrode (9). Since the impedance associated with the electrode–electrolyte interface must be proportional to the inverse of the area of the electrode, $4/\pi d^2$, it can always be made to dominate the constriction resistance by making the diameter sufficiently small. At 4 kHz with an electrode of $\approx 10^{-3}$ cm^2, the real part of the impedance of the electrode, the faradaic resistance, is several times larger than the constriction resistance. Under these conditions, the activities of anchored cells are clearly revealed. If instead two large electrodes had been used, the solution resistance would have masked the measurement, and the presence of cells would be barely detectable. The lower portion of Fig. 1 shows measured fluctuations in both the in-phase and out-of-phase voltage as a function of time for electrodes covered with a confluent layer of WI-38 VA13 cells.

The model used to calculate the specific impedance (the impedance for a unit area) of a cell-covered electrode as a function of the frequency, ν, is shown in Fig. 2. It is based on the measured specific impedance, $Z_n(\nu)$, of a cell-free electrode, the specific impedance, $Z_m(\nu)$, through the cell layer (i.e., mainly the capacitance of the upper and lower cell membranes in series) and the resistivity, ρ, of the tissue culture medium. The cells have been approximated as circular disks (not a limiting approximation) of radius r_c. We have assumed that the current flows radially in the space formed between the ventral surface of the cell and the substratum and that the current density under the cells does

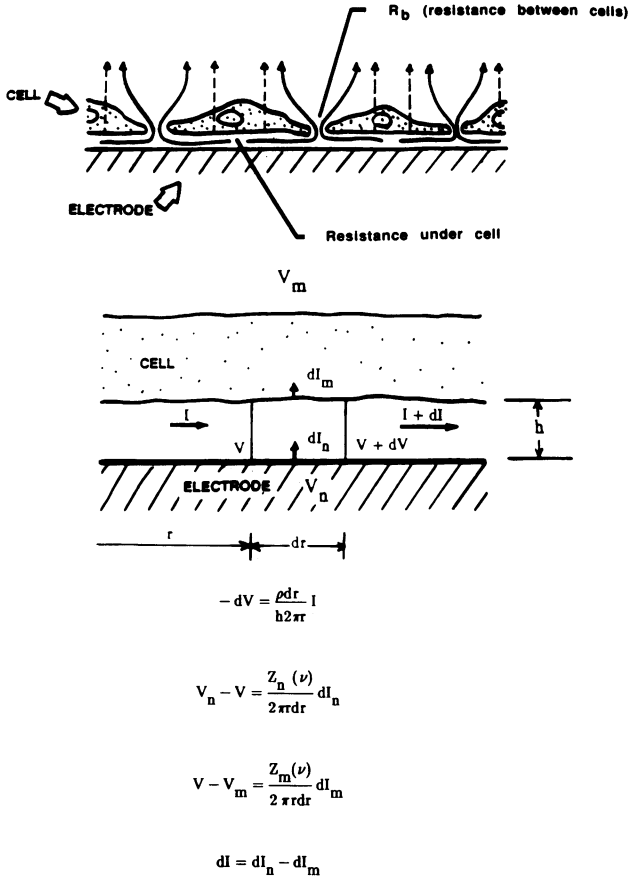

FIG. 2. Diagram of the cells in tissue culture emphasizing the spaces between the cell and the substratum. Calculated resistance is due to the current flow under the cells and an additional resistance because the current must flow out between the cells. Broken line represents capacitive current flow through the cell membranes. The cells are regarded as disk shaped when viewed from the top. The schematic side view diagram of cells is useful in constructing the differential equations. Here ρ is the resistivity of the solution, $Z_n(\nu)$ is the specific impedance of the electrode–electrolyte interface, and $Z_m(\nu)$ is the specific membrane impedance of the cells. If the capacitance of a single cell membrane is C, then for the intact cell, $Z_m = -i/2\pi\nu(C/2)$. In all calculations C is set at 1 μF/cm^2.

not change in the z direction. The equations in Fig. 2 can be combined to yield

$$\frac{d^2V}{dr^2} + \frac{1}{r}\frac{dV}{dr} - \gamma^2 V + \beta = 0,$$

where

$$\gamma^2 = \frac{\rho}{h}\left(\frac{1}{Z_n} + \frac{1}{Z_m}\right),$$

and

$$\beta = \frac{\rho}{h}\left(\frac{V_n}{Z_n} + \frac{V_m}{Z_m}\right),$$

where V_n is the potential of the electrode and V_m is the potential measured in the solution just outside the cell layer, and h is the height of the space between the ventral surface of the cell and the substratum.

The solution of this equation is a sum of modified Bessel functions of first and second kind (10). By using proper boundary conditions, the specific impedance for a cell-covered electrode can be written as follows:

$$\frac{1}{Z_c} = \frac{1}{Z_n}\left(\frac{Z_n}{Z_n + Z_m} + \frac{\dfrac{Z_m}{Z_n + Z_m}}{\dfrac{i\gamma r_c}{2}\dfrac{I_0(\gamma r_c)}{I_1(\gamma r_c)} + 2R_b\left(\dfrac{1}{Z_n} + \dfrac{1}{Z_m}\right)}\right),$$

where I_0 and I_1 are modified Bessel functions of the first kind of order 0 and 1, and i is $\sqrt{-1}$. The answer is rather involved but straightforward to develop; a detailed derivation will be published elsewhere. Note that the solution depends on two parameters—R_b, the resistance between the cells for a unit area, and α defined by:

$$\gamma r_c = r_c\sqrt{\frac{\rho}{h}\left(\frac{1}{Z_n} + \frac{1}{Z_m}\right)} = \alpha\sqrt{\frac{1}{Z_n} + \frac{1}{Z_m}}.$$

Since $Z_n(\nu)$ is measured and $Z_m(\nu)$ is basically the impedance of two cell membranes in series (see Fig. 2), α and R_b are the only adjustable parameters in the preceding expression. The frequency dependence does not appear explicitly in the equation, as it is contained in the impedances $Z_n(\nu)$ and $Z_m(\nu)$.

Using this model to calculate the impedance of an electrode supporting a confluent layer of cells, Z_c, we first measure the impedance of a cell-free electrode at different frequencies. It is convenient to interpret the measured sample impedance as equivalent to that of a capacitor and a resistor in series as was first done by Warburg (11, 12) for electrolytic interfaces. This has been done for the results shown in Fig. 3 *A* and *B*. Since the constriction resistance is in series with this impedance, it can simply be subtracted from the total resistance to obtain the real resistive value of Z_n. After calculating Z_c, the constriction resistance is added back for comparison with the experimental results. The solid lines in Fig. 3 *C* and *D* display the normalized resistance and capacitance obtained from electrodes confluent with WI-38 VA13 and WI-38 cells by dividing with the corresponding quantities for the cell-free electrodes. The points for all panels in Fig. 3 are calculated values based on the model.

The best fit to the WI-38 VA13 data is obtained with α = 7 ohm$^{1/2}$·cm (note γr_c is unitless) and R_b = 1.1 ohm·cm^2. Both the average radius of the cells (11 μm) and the resistance of the tissue culture medium (54 ohm·cm) were obtained from independent measurements (data not shown). This gives an average calculated channel height (substratum to ventral cell surface) of 13.3 nm. The best fit for WI-38 data is obtained with α = 3.5 ohm$^{1/2}$·cm and R_b = 0.35 ohm·cm^2. These normal fibroblastic cells are larger than the transformed WI-38 VA13 cells, and by using an average measured radius of 16 μm, the average calculated channel height becomes 113 nm. Rather than model the cells as circular disks, we can treat them as rectangles with widths equal to the diameter used. This gives larger ventral distances of 32 and 285 nm for WI-38 VA13 and WI-38, respectively. The distances in both cases are in reasonable agreement with measurements obtained from interference reflection microscopy (13) but, as can be seen, are strongly dependent on the assumed cell shape. The relatively close proximity of the transformed cells to the substratum compared with the normal cells is, however, independent of the choice of cell shape in the model. The resistance of the cell layer used to fit the data is only on the order of 1 ohm·cm^2 but nevertheless is needed to get a good agreement with the experimental observations. This small value explains why it is difficult by conventional means to measure resistance of cell layers other than epithelial cells, where the value is ≈2 orders of magnitude greater (14).

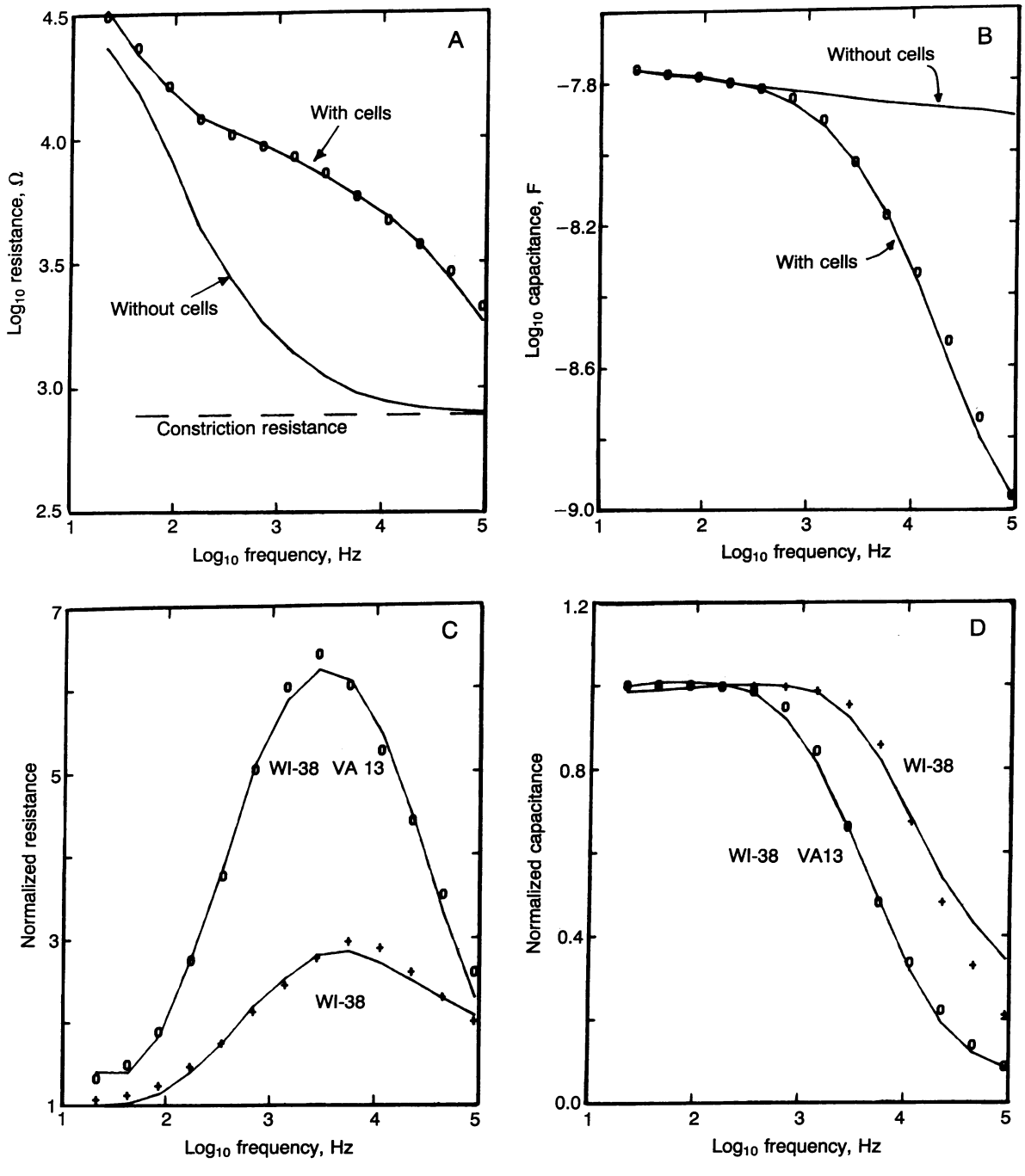

FIG. 3. Impedance as a function of frequency for a small electrode of area 1.06×10^{-3} cm^2. (*A*) Resistance of a cell-free electrode and the same electrode confluent with WI-38 VA13 cells. The points are the calculated values. Note that this is a log-log plot. (*B*) The same values for the observed capacitance. (*C*) For better sensitivity the normalized resistances are plotted, both for an electrode confluent with WI-38 VA13 cells and for an electrode with WI-38 cells. Points are calculated values; o, WI-38 VA13; +, WI-38. (*D*) The same for normalized capacitance.

It should be noted that the cells, of course, are neither circular nor rectangular, nor do they all have the same shape. This simple model shows, however, that the change in impedance due to a confluent cell layer stems from two sources: the current flow between the ventral surface of the cells and the substratum, and the resistance between cells.

Fig. 4*A* shows the first 2 min of data taken from Fig. 1. Here the equivalent resistance has been calculated from the data, representing the sample as a resistor and capacitor in series, and is normalized to the value at time 0. These are typical of fluctuations from an electrode with confluent WI-38 VA13 cells measured at 4 kHz. Fig. 4*B* shows the lack of fluctuations after a brief 10% formalin treatment to kill the cells. The measurements have been obtained with a digital lock-in amplifier, and the digital feature accounts for the steps in the curve. Again, since the electrode is confluent with cells, the measured fluctuations in the resistance cannot be ascribed to variations in the cell number that cover the electrode as would be the case from random walks of cells in sparse cultures. Instead, the fluctuations are due to the variations in the factors that make up α, or in the resistance between the cells, R_b. The calculated values of α or R_b that correspond to the experimental resistance changes are shown on the right hand ordinant of Fig. 4, assuming that each is exclusively responsible for the resistance change. Also marked on Fig. 4

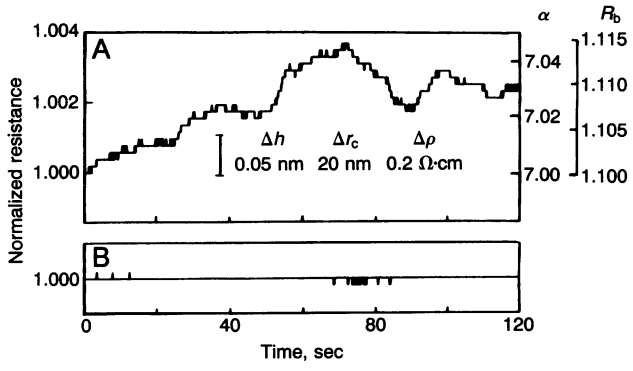

FIG. 4. Two minutes of resistance fluctuations for live (*A*) and formalin-treated (*B*) WI-38 VA13 cells. The digital amplifier used accounts for the steps in the curve. By calculation, it can be shown that the step height is consistent with a change in the average distance between the ventral surface of the cells and the electrodes of only 0.01 nm or a change in the cell radius of 4 nm.

is a bar showing the typical change in the calculated resistance that would result if only one of the three variables in α had changed by the value listed. (Note that the change in resistance is not strictly linear in these values.)

It is not clear from these results whether the measured resistance fluctuations are due to small variations in α or R_b; however, from partially covered electrodes, where R_b must be 0, it can be estimated that they are of roughly equal importance (data not shown). What is clear, however, is the exquisite sensitivity of the experiment. It should be noted that large fluctuations in the electrical impedance can be observed when, simultaneously, no discernible change is seen with an optical microscope. This is not surprising because changes of nanometers in the cell diameter or subnanometer changes in the distance between the ventral surface of the cell and the substrate will significantly affect the measured impedance. We refer to this subtle aspect of cell motility as micromotion. It should be pointed out here that, at the present amplifier magnification, there is essentially no problem with electrical noise as can be seen from the formalin-treated cells. It is also clear that the fluctuations are associated with the living cells and in no way are an artifact of the measurement.

While theory and experiment agree very well, one small difficulty should be pointed out. Experimentally, the capacitance at low frequency increases for long-term (a few days) experiments by 5–10% for confluent electrodes. The increase varies arbitrarily between electrodes in a single experiment and from experiment to experiment. Because the cells form adhesion plaques (focal contacts) with the electrodes, the measured capacitance is expected to be 5–10% smaller than that for the cell-free electrode. The reason for the increase in capacitance is unclear but it offers no problem for the time scale of the experimental results described in this paper. Unfortunately, until this problem is understood, the experimental method cannot be used to measure the sizes of the adhesion plaques between the cells and the substratum.

A confluent electrode contains on the order of 50 cells; it is, however, possible to measure the effect of a single cell on the electrode. This is experimentally more difficult. We are also examining how various external factors, such as temperature, pH, or addition of drugs will affect the motion of cells at this length scale. The inherent simplicity of the system and the sensitivity of these measurements offers great promise for many tissue culture applications.

This work was carried out in part pursuant to a contract with the National Foundation for Cancer Research.

1. Abercrombie, M. (1982) in *Cell Behavior*, eds. Bellairs, R., Curtis, A. & Dunn, G. (Cambridge Univ. Press, London), pp. 10–48.
2. Partin, A. W., Isaac, J. T., Treiger, B. & Coffey, D. S. (1988) *Cancer Res.* **48**, 6050–6053.
3. Partin, A. W., Schoeniger, J. S., Mohler, J. L. & Coffey, D. S. (1989) *Proc. Natl. Acad. Sci. USA* **86**, 1254–1258.
4. Brady-Kalnay, S. M., Soll, D. R. & Brackenbury, R. (1991) *Int. J. Cancer* **47**, 560–568.
5. Giaever, I. & Keese, C. R. (1989) *Physica D* **38**, 128–133.
6. Giaever, I. & Keese, C. R. (1986) *IEEE Trans. Biomed. Eng.* **33**, 242–247.
7. Giaever, I. & Keese, C. R. (1984) *Proc. Natl. Acad. Sci. USA* **81**, 3761–3764.
8. Heaysman, J. E. M. & Pegrum, S. M. (1982) in *Cell Behavior*, eds. Bellairs, R., Curtis, A. & Dunn, G. (Cambridge Univ. Press, London), pp. 49–76.
9. Holm, R. (1946) *Electrical Contacts* (Almqvist & Wiksells, Uppsala), p. 16.
10. Hildebrand, F. B. (1948) *Advanced Calculus for Engineers* (Prentice–Hall, Englewood Cliffs, NJ), pp. 152–181.
11. Warburg, E. (1901) *Ann. Phys.* **6**, 125–135.
12. Onaral, B., Sun, H. H. & Schwan, H. P. (1984) *IEEE Trans. Biomed. Eng.* **31**, 827–832.
13. Izzard, C. S. & Lochner, L. R. (1980) *J. Cell Sci.* **42**, 81–116.
14. Fuller, S., von Bonsdorff, C. H. & Simons, K. (1984) *Cell* **38**, 65–77.